

# Ultra-Compact Micromachined Beam-Steering Antenna Front-End for High-Resolution Sub-Terahertz Radar

Umer Shah, Adrian Gomez, and Joachim Oberhammer

School of Electrical Engineering and Computer Science, KTH Royal Institute of Technology, 100 44 Stockholm, Sweden

**Abstract**—This paper reports on an ultra-compact sub-THz frequency based beam-steering radar antenna front-end implementation utilizing a micromachined parallel-plate waveguide based leaky wave antenna. At a size of only  $24 \times 24 \times 0.9$  mm<sup>3</sup>, the beam-steering front-end antenna has a 28 dBi gain and a 45° field of view for scanning over 220-300 GHz. As compared to a theoretical range resolution of 6.8 mm, a range resolution of 1.2 cm was experimentally verified for 2.5 cm large targets separated by 8°. Furthermore, this paper shows a signal processing technique for frequency-steerable antennas which achieves high angular target separation by splitting the measurement frequency range into sub-sections to isolate similar slant range close-proximity targets into different frequency spaces.

## I. INTRODUCTION

**R**ADAR implementations at sub-terahertz frequencies offer significant advantages in terms of wide instantaneous bandwidth, smaller antenna size and higher range resolution, and better velocity and angular discrimination [1]. Range and angular resolution are the minimum longitudinal and angular distances, respectively, between two targets in close proximity that are still distinguishable by the radar. In the signal-processing each signal return is modeled by adding the individual power levels of the sinc function envelope and multiple targets can only be resolved if the targets are spaced by at least  $1/\text{bandwidth}$  in the time response, limiting the achievable range resolution to  $\Delta R = c/2B$  with  $c$  being the speed of light and  $B$  the bandwidth. The angular resolution, on the other hand depends on the beamwidth of the antenna. High angular resolution requires the antenna to have a pencil shaped beam with a narrow beamwidth and a high gain. Moreover, to achieve wide field of view, the narrow antenna beam needs to be steered.

Solid state sources at sub-terahertz frequencies have limited output power and thus very limited range, decreasing further with increasing frequency [2]. Frequency modulated continuous wave (FMCW) radars can deliver higher mean power on target as compared to pulsed radars because of the 100% duty cycle of the waveform. This makes the FMCW radar a popular choice for sub-terahertz radar implementations. FMCW radar measures the travel time of a signal directly from the difference in frequency between the transmit and the receive signals [3]. The IF bandwidth required by FMCW radars is typically also small as compared to the frequency sweep bandwidth and I/Q demodulation is typically not needed. A stepped-frequency continuous wave (SFCW) radar uses a discretized version of a FMCW radar waveform which comprises of single frequency tones stepped by frequency intervals of  $\Delta f$  hertz across a bandwidth  $B$ . SFCW radars measure the travel time of the reflected signals by measuring the phase difference between the transmit and

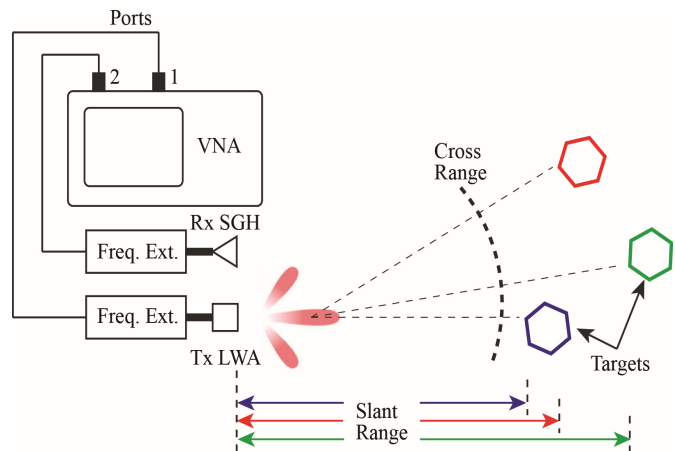
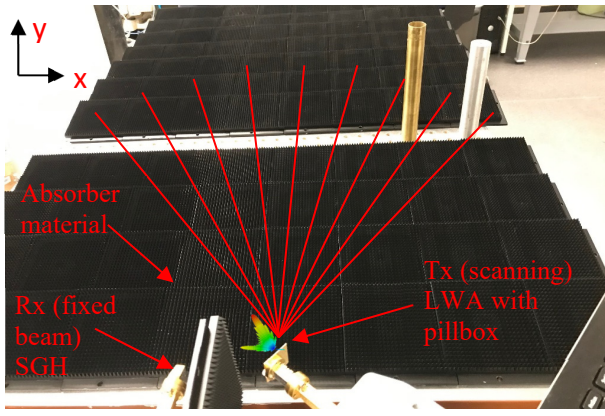


**Fig. 1.** Measurement setup utilizing the Vector Network Analyzer (VNA) with 220-330 GHz frequency extenders, the micromachined parallel plate waveguide (PPW) leaky wave antenna (LWA) as transmit antenna and a standard gain horn (SGH) as receive antenna making the radar front-end for range measurement and angular resolution of multiple targets in close proximity.

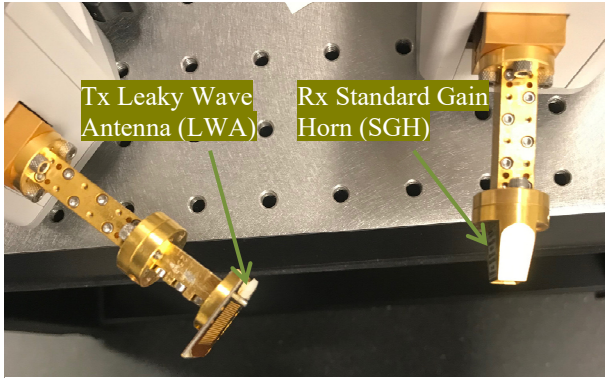
the receive signals at each frequency step, and thus require an I/Q demodulation. The stepped-frequency waveform removes the requirements for wide instantaneous bandwidth and high sampling rates of other radar waveforms by making a steady-state continuous wave measurement as the target is illuminated at discrete frequency steps. However, the frequency quantization steps leads to range ambiguity  $R_{un} = c/2\Delta f$  which depends on the quantization frequency step size  $\Delta f$ . High range resolution is, as for any radar waveform, achieved by utilizing a large overall bandwidth  $B$  but for achieving large angular resolution, special post processing techniques are required together with the requirement of narrow antenna beamwidth and high antenna gain.

## II. IMPLEMENTATION

We propose for the first time an ultra-compact implementation of sub-terahertz radar front-end antenna. The measurement setup is shown in Fig. 1. The frequency beam steering frontend is based on a parallel plate waveguide (PPW) leaky wave antenna (LWA) operating between 220 to 300 GHz and provides a continuous beam scanning in a  $45^\circ$  field of view (FoV) [4]. The LWA generates an unbound radiating mode with the periodic slot array on the top plate of the PPW [5]. This combination provides a pencil shaped beam with a realized gain up to 28 dBi and 80% radiation efficiency. The high gain provided by the LWA is a requirement for achieving high angular resolution in the radar system. The antenna is fabricated at KTH by silicon micromachining in a low loss waveguide technology [6], resulting in a very compact beam-steering antenna frontend with a total size of  $24 \text{ mm} \times 24 \text{ mm} \times 0.9 \text{ mm}$ . The prototype measurements utilize a Vector



(a)



(b)

**Fig. 2.** Image of the measurement setup: (a) for slant range measurement of two targets in close proximity; and (b) close-up of the LWA and SGH mounted on the waveguide flange of the frequency extenders.

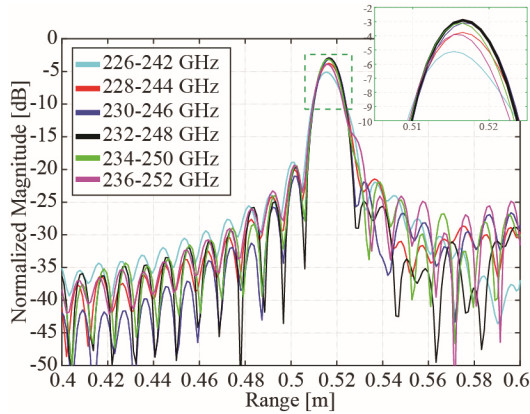


**Fig. 3.** Measured slant range data for a single target illuminated by the LWA with a FFT of 16 GHz sub-bands swept across the total bandwidth. Accurate slant range information is obtained when the target is illuminated by the main-lobe achieving maximum reflectivity.

Network Analyzer (VNA) based Tx/Rx signal feeding and a SFCW radar waveform. A Rohde & Schwarz ZVA-24 VNA with ZC330 frequency extenders is used to illuminate the targets and to measure the reflections at discrete frequency steps. The LWA is mounted on the transmit port of the VNA and a standard gain horn (SGH) is mounted on the receive port as shown in Fig. 2. The metal table in front of the antennas is covered by absorbers, as shown in Fig. 2a. The sampling is done at steady state reflectivity as the target is illuminated at discrete frequencies. The range resolution depends on the bandwidth for which the LWA illuminates the target while the

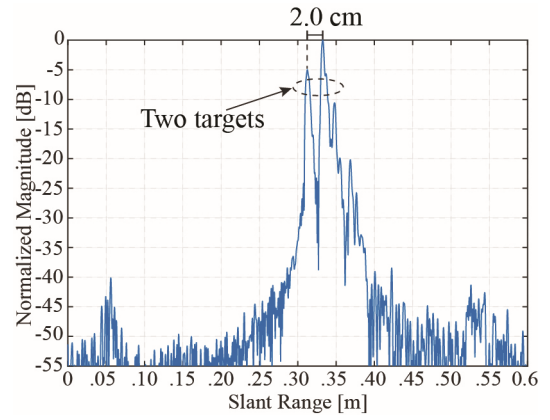


**Fig. 4.** Measured range data for two targets in close proximity (2 cm apart in slant range). A full bandwidth FFT is performed in the post-processing clearly separating the two targets.

Tx frequency is swept. The angular resolution depends on the beamwidth of the main antenna lobe together with the signal processing technique of splitting the measurement frequency band into smaller sections to separate the illumination of targets in frequency and thus in angle. The signal processing is done offline after the frequency scanning, but only requires inverse Discrete Fourier Transformation (iDFT) of the band or sub-bands, which can be implemented in real time in a radar system.

### III. RESULTS

In the first experiment, measurements are performed on a single target placed in front of the radar measurement setup. In the post-processing, the data of 16 GHz sub-bands is separated from the total bandwidth (220-300 GHz) while computing the inverse Fourier transform across each individual sub-band. The most accurate target slant range information in comparison with the full band iDFT is attained at the maximum reflectivity sub-band of 232-248 GHz as shown in Fig. 3. Furthermore, the same slant range information is extracted from the sub-band 228-244 GHz, 230-246 GHz and 234-250 GHz. The slant range is distorted for the other sub-bands where the reflectivity is reduced and the target positioning is not accurate since the target is no longer illuminated by the main-lobe but rather by the radiation pattern artifacts around the main-lobe and the backlobe typical for non-perfectly terminated leaky-wave antennas. The target is illuminated for at least 22 GHz by the main-lobe, depending on the angular position since the main-lobe beam width is frequency dependent. This result in a theoretical range resolution of 6.8 mm. For measuring the range resolution value, two targets (metal rods) are placed in close proximity and a full bandwidth iDFT is performed in the post-processing. Fig. 4 shows that the targets are 2 cm apart and can clearly be separated in the post-processing. The angular resolution is limited by the half power beam width (HPBW) (6-15° depending on pointing direction). Two exemplary targets spaced 8° (angular) and 1.2 cm (longitudinal) apart, at a range of 52 cm, cannot be clearly distinguished in range with conventional stepped-frequency CW with full-bandwidth iDFT, as shown in Fig. 5a. The HPBW of the main lobe for the direction of these targets is 9°. In contrast to that, these close-proximity targets can clearly be resolved by the signal

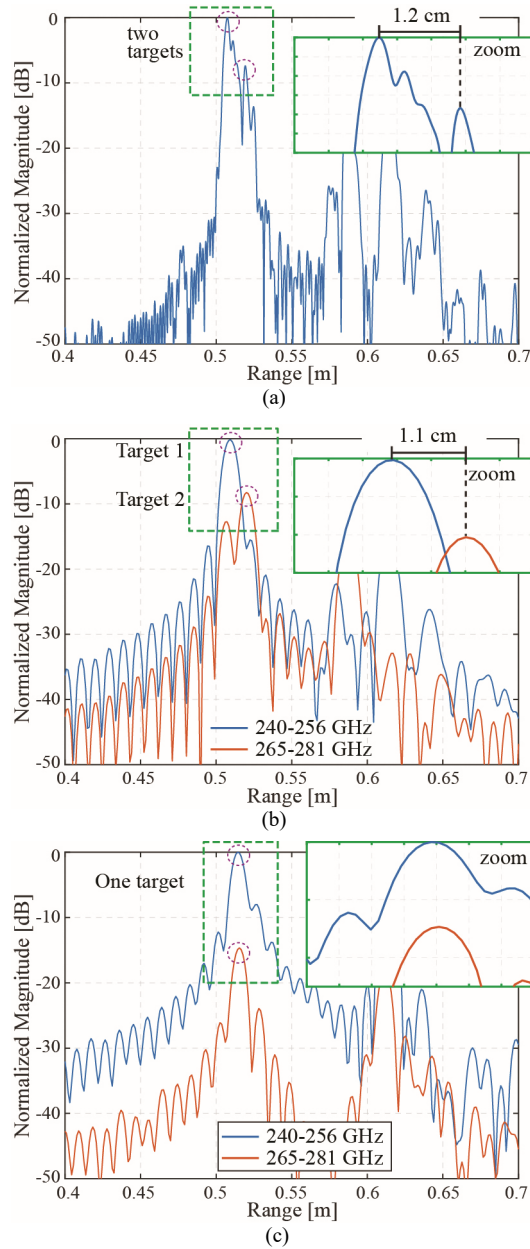


**Fig. 5.** Measurement results for two targets placed at 1.2 cm distance: (a) Range data for full band; the two targets are not clearly distinguishable; (b) range data for the sub-band signal processing clearly able to discriminate the two targets; (c) range data for a single target sub-band signal processing clearly shows only one target in the two sub-bands. The HPBW of the main lobe at the direction of the two targets is  $9^\circ$ .

processing method proposed in this paper, i.e. by splitting the total bandwidth into 16 GHz sub-bands with individual sub-band iDFT, as shown in Fig. 5b. The choice of the split frequency between the sub-bands associated to the two targets can be optimized simply by observing the target separation in the two iDFT results. To validate the results, a single target was also measured and the total bandwidth is split into the same 16 GHz sub-bands as used for two targets with individual sub-band iDFT. The result only shows one target in both sub-bands, since the target appearing in both sub-bands is at the same range, as shown in Fig. 5c. In one of the bands the single target is visible but strongly attenuated since it is only exposed to sidelobes in this band.

#### IV. SUMMARY

This paper shows an ultra-compact,  $24 \times 24 \times 0.9 \text{ mm}^3$  large, sub-THz frequency based beam-steering antenna radar front-end implementation utilizing a micromachined leaky wave antenna operating at 220-300 GHz with a  $45^\circ$  field of view. A signal processing technique is introduced that splits the measurement frequency range into smaller sections to separate similar slant range or close-proximity targets into different frequency sub-bands to achieve high angular resolution. Experimentally, two close-proximity, 2.5 cm large targets at a slant range distance of 1.2 cm and an angular spacing of  $8^\circ$ , which cannot be discriminated in range by conventional full-band iDFT, could clearly be separated with this method.

#### ACKNOWLEDGMENT

This work was funded by the CAR2TERA project of the European Union's Horizon 2020 research and innovation programme under grant agreement No. 824962.

#### REFERENCES

- [1]. J. Grajal, et. al., "Compact radar front-end for an imaging radar at 300 GHz," *IEEE Trans. THz Sci. Technol.*, vol. 7, no. 3, pp. 268–273, Mar. 2017.
- [2]. G. Chattopadhyay, "Technology, capabilities, and performance of low power terahertz sources," *IEEE Trans. Terahertz Sci. Technol.*, vol. 1, no. 1, pp. 33–53, Sep. 2011.
- [3]. M. Skolnik, *Introduction to Radar Systems*, 2 ed. New York: McGraw Hill Book Co., 1980.
- [4]. Adrian Gomez-Torrent, Maria Garcia-Vigueras, Laurent Le Coq, Adham Mahmoud, Mauro Ettorre, Ronan Sauleau, and Joachim Oberhammer, "A Low-Profile and High-Gain Frequency-Beam-Steering sub-THz Antenna Enabled by Silicon Micromachining," submitted for publication.
- [5]. A. A. Oliner, "Leaky-wave antennas," in *Antenna engineering handbook* (R. C. Johnson, ed.), pp. 280–338, McGraw-Hill Professional, 1992.
- [6]. B. Beuerle, et. al., "A very low loss 220-325 GHz silicon micromachined waveguide technology," *IEEE Trans. on THz Sci. Tech.*, vol. 8, pp. 248-250.